

Article

## Solid-State NMR Studies of Aminocarboxylic Salt Bridges in L-Lysine Modified Cellulose

Ricardo Manriquez, Fernando A. Lopez-Dellamary, Jaroslaw Frydel, Thomas Emmler, Hergen Breitzke, Gerd Buntkowsky, Hans-Heinrich Limbach, and Ilja G. Shenderovich

*J. Phys. Chem. B*, **2009**, 113 (4), 934-940 • DOI: 10.1021/jp8081968 • Publication Date (Web): 31 December 2008

Downloaded from <http://pubs.acs.org> on February 3, 2009

### More About This Article

Additional resources and features associated with this article are available within the HTML version:

- Supporting Information
- Access to high resolution figures
- Links to articles and content related to this article
- Copyright permission to reproduce figures and/or text from this article

[View the Full Text HTML](#)

## Solid-State NMR Studies of Aminocarboxylic Salt Bridges in L-Lysine Modified Cellulose

Ricardo Manríquez,<sup>†,‡</sup> Fernando A. López-Dellamary,<sup>‡</sup> Jaroslaw Frydel,<sup>†</sup> Thomas Emmler,<sup>†</sup> Hergen Breitzke,<sup>§</sup> Gerd Buntkowsky,<sup>§</sup> Hans-Heinrich Limbach,<sup>†</sup> and Ilja G. Shenderovich<sup>\*,†,‡,#</sup>

*Institut für Chemie und Biochemie, Freie Universität Berlin, Takustrasse 3, D-14195 Berlin, Germany; Departamento de Madera, Celulosa y Papel, CUCEI, Universidad de Guadalajara, Kilómetro 15.5, Carretera Guadalajara-Nogales, Guadalajara, C.P. 45020, Jalisco, México; Institut für Physikalische Chemie, Universität Jena, Helmholtzweg 4, D-07743, Jena, Germany; and V.A. Fock Institute of Physics, St.Petersburg State University, Ulianovskaya 1, 198504 St. Petersburg, Russian Federation*

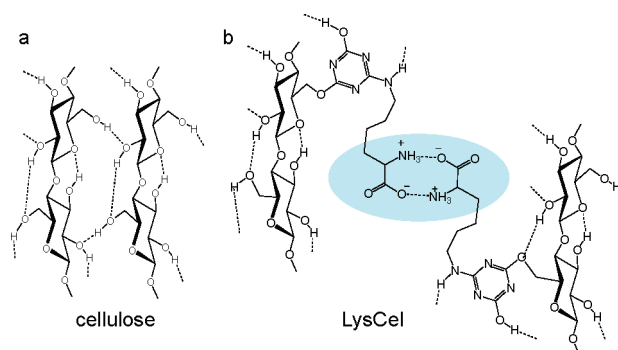
Received: September 15, 2008; Revised Manuscript Received: November 10, 2008

LysCel is a cellulose-based material in which L-lysine molecules are grafted with their amino side chains to the cellulose hydroxyl groups. This modification increases considerably the mechanical strength and resistance of cellulosic structures toward water. It has been attributed to the formation of double salt bridges between lysine aminocarboxyl groups in the zwitterionic state. In order to characterize this unusual structure, we have performed high-resolution solid-state <sup>15</sup>N and <sup>13</sup>C CPMAS NMR experiments on LysCel samples labeled with <sup>15</sup>N in the α-position or ε-position. Furthermore, <sup>13</sup>C–<sup>15</sup>N REDOR experiments were performed on LysCel where half of the aminocarboxyl groups were labeled in 1-position with <sup>13</sup>C and the other half in α-position with <sup>15</sup>N. The comparison with the <sup>13</sup>C and <sup>15</sup>N chemical shifts of L-leucine lyophilized at different pH shows that the aminocarboxyl groups of LysCel are indeed zwitterionic. The REDOR experiments indicate distances of about 3.5 Å between the carboxyl carbon and the nitrogen atoms of different aminocarboxyl groups, indicating that the latter are in close contact with each other. However, the data are not compatible with isolated aminocarboxyl dimers but indicate the assembly of zwitterionic aminocarboxyl dimers either in a flat ribbon or as tetramers, exhibiting similar intra- and interdimer <sup>13</sup>C···<sup>15</sup>N distances. This interaction of several aminocarboxyl groups is responsible for the zwitterionic state, in contrast to the gas phase, where amino acid dimers exhibiting two OHN hydrogen bonds are neutral.

## Introduction

Cellulose constitutes a very important renewable-resource-based raw material for paper production. It is a linear polysaccharide in which the anhydroglucose repeat units (AGU's) are linked together through β-1,4 glycosidic bonds. The cellulose chains agglomerate to linear strands called microfibrils which form themselves larger assemblies. The latter constitute the cell walls of the higher plants. This polymeric order, chain length, and chains assembly confer to this material excellent mechanical properties and insolubility in water at different pH at ordinary temperatures.<sup>1,2</sup> The current accepted postulate for the stability of cellulosic structures is the formation of intra- and intermolecular hydrogen bonds as illustrated in Scheme 1a.<sup>3,4</sup>

However, the tensile strength of paper which is made of cellulose fibers is poor. It can take up water which breaks the hydrogen bond interactions between them.<sup>5</sup> Increasing the tensile strength of paper by improving the strength of interfiber bonding constitutes, therefore, an important field of research.<sup>6</sup> Some attempts have been made to introduce ionic interactions to enhance the tensile strength in paper. As the fibers of cellulose are considered charged negatively, positive charges were introduced either by addition of some fillers, such as cationic starch<sup>7</sup> or polyelectrolytes,<sup>8–11</sup> or by grafting quaternary ammonium groups to the cellulose fibers.<sup>12</sup>

SCHEME 1: Postulated Structure of Lysine-Modified Cellulosic Fibers (LysCel) According to Ref 6<sup>a</sup>

<sup>a</sup> Zwitterionic aminocarboxyl dimers are supposed to glue the fibers together.

On the other hand, amino acids constitute renewable-resource-based materials. For example, the annual world market of lysine is of the order of 10<sup>8</sup> kg.<sup>13</sup> Therefore, Allan et al.<sup>6</sup> have grafted the amino side chain of L-lysine to the hydroxyl groups of solid cellulose fibers using the dichloro-*s*-triazine chemistry of the commercially available Procion dyes (Scheme 1b). As compared to nonmodified cellulose, a considerable wet-strength improvement of 30–35% was observed for the lysine-modified cellulose,<sup>6,14</sup> called LysCel throughout this paper. Allan et al.<sup>6,14</sup> attributed the increase of the interfiber binding strength of LysCel to the formation of zwitterionic dimers between the aminocarboxyl residues of the grafted lysine as depicted in Scheme 1b.

\* To whom correspondence should be addressed. E-mail: shender@chemie.fu-berlin.de.

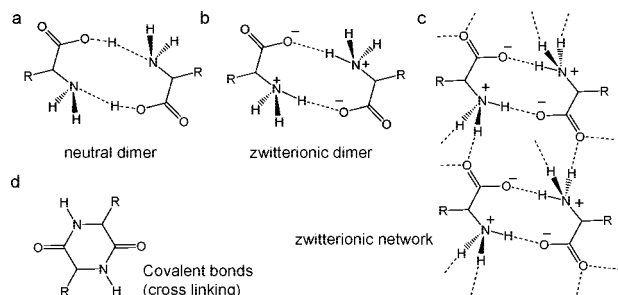
<sup>†</sup> Freie Universität Berlin.

<sup>‡</sup> Universidad de Guadalajara.

<sup>§</sup> Universität Jena.

<sup>#</sup> St. Petersburg State University.

**SCHEME 2: Neutral Dimers (a), Zwitterionic Dimers (b), and Zwitterionic Networks Exhibiting OHN–Hydrogen Bonds between Aminocarboxyl Groups of Amino Acids (c) As Possible Binding Motifs in LysCel;<sup>a</sup> (d) Potential Cross-Linking in LysCel as the Result of the Formation of a Cyclic Dipeptide**



<sup>a</sup> The network structure shown is derived from the crystal structure of glycine.<sup>25</sup>

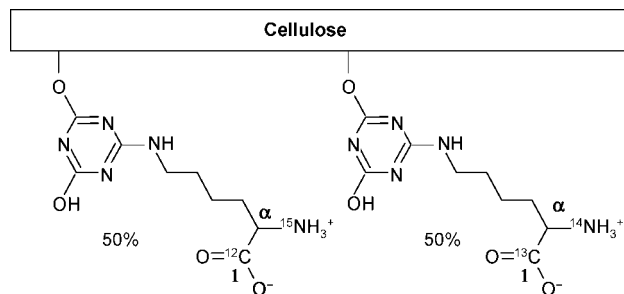
However, this structure raises several questions. Indeed, in aqueous solutions at pH around 7, near their isoelectric point (pI), amino acids are present in their zwitterionic form which is stabilized by surrounding water molecules.<sup>15</sup> In organic solvents, the solubility of amino acids is not large enough to study their dimerization. In the gas phase, zwitterionic dimers are not stable.<sup>16–19</sup> Hobza et al.<sup>20</sup> have performed *ab initio* calculations of isolated glycine dimers and found 22 different structures stabilized mostly by hydrogen bonds. Among the dimers exhibiting two OHN–hydrogen bonds only the neutral form was found (Scheme 2a), but not the postulated zwitterionic form depicted in Scheme 2b. Thus, the structure of such a dimer is unknown. The attraction between the electrical charges could lead to very nonlinear hydrogen bonds as indicated schematically in Scheme 2b.

The reason for the absence of zwitterionic OHN–hydrogen bonds in the gas phase has been discussed previously for the case of ammonia–acid complexes. In order to convert a neutral hydrogen bond  $A-H\cdots B$  into the corresponding zwitterionic form  $A^-\cdots H-B^+$ , external electric fields are required<sup>21</sup> which can be produced by solvent dipoles or via the assembly of many hydrogen bridges of the same type. Thus, amino acids generally crystallize as zwitterions; however, an inspection of the reported crystal structures of glycine,<sup>22–25</sup> valine,<sup>26</sup> leucine,<sup>27</sup> and cocrystals of leucine–valine<sup>28</sup> shows that complex hydrogen bond networks prevail in which the zwitterionic forms are stabilized. An example for such a network is depicted schematically in Scheme 2c which consists of a ribbon which may be part of a sheet or of a three-dimensional assembly. Embedded in cellulose, such a ribbon reminds one of the nucleic acid bases which hold the polyribosephosphate chains together. Thus, such a ribbon could also be responsible for the mechanical strength of LysCel.

Finally, the observed mechanical strength of this material could also be the result of cross-linking via the formation of a cyclic dimeric peptide anhydride as depicted in Scheme 2d. The formation of such a cyclic anhydride has already been reported to occur on the surface of polyhydroxylated systems such as alumina.<sup>29,30</sup> Such a cross-linking is irreversible and may constitute a problem for the handling of LysCel.

In order to characterize LysCel in more detail, we have used solid-state NMR spectroscopy which constitutes an important tool to study acid–base properties of polymeric fibers.<sup>31</sup> For that purpose, we synthesized different isotopically labeled LysCel samples, i.e., LysCel labeled with <sup>15</sup>N either in the  $\alpha$ -

**SCHEME 3: Chemical Structure of [<sup>13</sup>C/<sup>15</sup>N]LysCel Used for <sup>13</sup>C CPMAS and <sup>13</sup>C–<sup>15</sup>N REDOR NMR Experiments**



or the  $\epsilon$ -position ( $[\alpha\text{-}^{15}\text{N}]\text{LysCel}$  and  $[\epsilon\text{-}^{15}\text{N}]\text{LysCel}$ , respectively), and a sample where half of the aminocarboxyl groups were labeled with  $1\text{-}^{13}\text{C}$  in the carboxylic acid sites and the other half with  $^{15}\text{N}$  in the amino sites ( $[\text{LysCel}/^{15}\text{N}]\text{LysCel}$ ) (Scheme 3).

Our first goal was to demonstrate the presence of lysine groups in LysCel, to exclude the cyclic peptide formation, and to inspect the protonation states of the aminocarboxyl groups by solid-state NMR. This task was facilitated by the observation that the  $^{13}\text{C}$  and  $^{15}\text{N}$  chemical shifts of carboxylic and amino groups are very sensitive to their hydrogen bonding and protonation states.<sup>32,33</sup> However, in order to assist the interpretation, we performed  $^{13}\text{C}$  and  $^{15}\text{N}$  NMR measurements on solid L-leucine where the protonation states of the aminocarboxyl groups were varied by lyophilization at different pH.

Our second goal was to obtain information about the arrangement of the aminocarboxyl groups in  $[\text{LysCel}/^{13}\text{C}/^{15}\text{N}]\text{LysCel}$  using  $^{13}\text{C}$ – $^{15}\text{N}$  REDOR (rotational echo double resonance) NMR.<sup>34,35</sup> This method allows one to measure dipolar couplings and hence distances between selected spins, here between the  $^{13}\text{C}$  and  $^{15}\text{N}$  spins contained in different aminocarboxyl groups. In particular, we tried to detect the average number of amino nitrogens in close proximity to the  $1\text{-}^{13}\text{C}$  carbon of a given group.

This paper is organized as follows. After an experimental section in which materials and methods are described, the results are presented and discussed.

## Materials and Methods

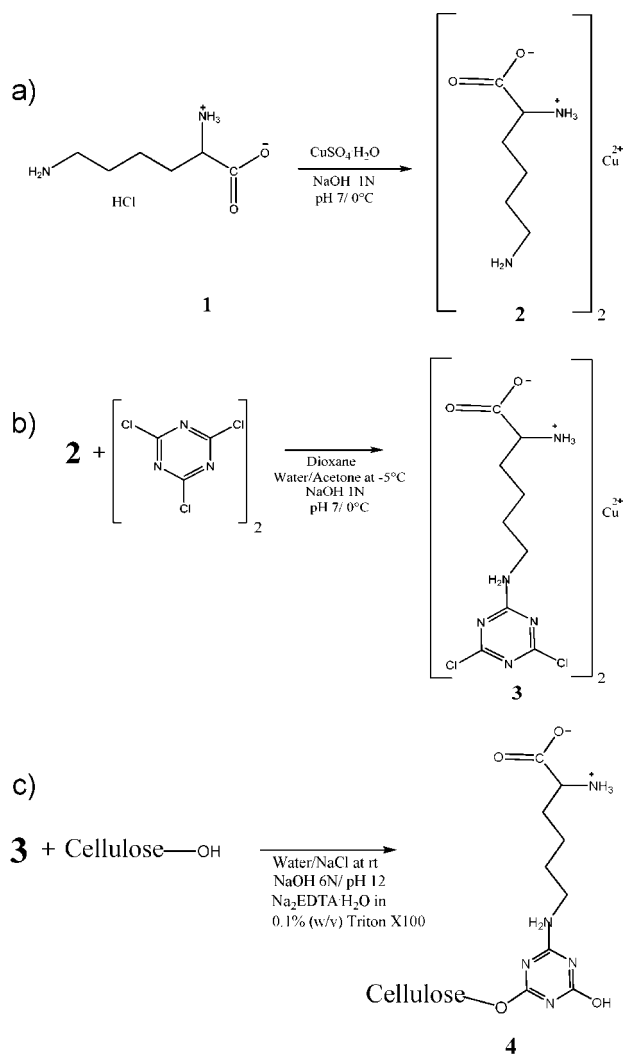
**Materials.** Samples were prepared using powdered cellulose from spruce (Fluka) with a fiber length of 0.02–0.15 mm and a degree of polymerization about 560. Ethylenediaminetetraacetic acid disodium salt dihydrate ( $\text{Na}_2\text{EDTA}\cdot 2\text{H}_2\text{O}$ ) 99.0%, L-lysine monohydrochloride 98%, Triton X-100, and cyanuric chloride 99% were supplied by Sigma-Aldrich. L-Leucine 98% was provided by Merck.  $\alpha\text{-}^{15}\text{N}$ - (95.99%),  $\epsilon\text{-}^{15}\text{N}$ - (98%), and  $1\text{-}^{13}\text{C}$  (99%) enriched L-lysines were purchased from Cambridge Isotope Laboratories, Inc. Cyanuric chloride was previously purified by recrystallization from hot  $\text{CCl}_4$ .

**Syntheses.** The synthetic procedures are described in detail in the Supporting Information.

**Lyophilized L-leucine.** These samples were prepared dissolving 0.2 g of L-leucine in 20 mL of bidistilled water. Eight samples with different pH's in the range from 2 to 13 were adjusted with solutions of HCl (1 N, 0.1 N) or NaOH (1 N, 0.1 N). The samples were frozen at  $-20\text{ }^\circ\text{C}$  and lyophilized.

**LysCel.** The modification of cellulose was carried out following the procedure of Allan et al.<sup>6</sup> For that purpose, L-lysine hydrochloride (**1**) was first converted into the copper complex **2** according to Scheme 4a, and then converted into  $\text{Cu}(\text{N}6\text{-}(4,6\text{-}$

## SCHEME 4: Synthesis of LysCel According to Ref 6



dichloro-1,3,5-triazin-2-yl)-L-lysine)<sub>2</sub> (**3**) (Scheme 4b). In the next step (Scheme 4c), cellulose suspended in water was let to react with **3**. The molar ratio was such that half of anhydro-glucose units (AGU) were modified. After the copper ions were removed with EDTA, the product was extensively washed with water at pH 7. The presence of amino acids in each LysCel sample was determined qualitatively by means of the classical method of ninhydrine and quantitatively by elemental analysis.

**Isotopically Labeled LysCel.**  $[\alpha\text{-}^{15}\text{N}]$ LysCel and  $[\varepsilon\text{-}^{15}\text{N}]$ LysCel were prepared according to the same procedure using the corresponding selectively labeled L-lysine isotopologues. For the REDOR experiments, a sample was synthesized using a 1:1 mixture of  $[\alpha\text{-}^{15}\text{N}]$ lysine and  $[1\text{-}^{13}\text{C}]$ lysine, leading to  $[1\text{-}^{13}\text{C}, \alpha\text{-}^{14}\text{N}]_{0.5}[1\text{-}^{12}\text{C}, \alpha\text{-}^{15}\text{N}]_{0.5}$ -LysCel which we will abbreviate as  $[^{13}\text{C}/^{15}\text{N}]$ LysCel. The chemical structure of the latter is illustrated in Scheme 3. This sample was synthesized using 0.5 equiv of  $\alpha\text{-}^{15}\text{N}$ -L-lysine, 0.5 equiv of  $1\text{-}^{13}\text{C}$ -L-lysine, and 2.5 equiv (based on AGU) of cellulose.

**NMR Measurements. Cross Polarization (CP) Experiment.**  $^{15}\text{N}$  and  $^{13}\text{C}$  CPMAS NMR experiments were performed at room temperature on a Varian CMX 300 spectrometer operating at 30.42 MHz for  $^{15}\text{N}$  and 75.46 MHz for  $^{13}\text{C}$  frequencies under a magnetic field of 7 T wide bore magnet. The cellulose samples were packed into a 6 mm  $\text{ZrO}_2$  rotor and measured in a Chemagnetics MAS probe with the spinning speed set to 7 kHz. For the CPMAS  $^{15}\text{N}$  NMR experiment, the  $90^\circ$  pulse width was

about  $5.5 \mu\text{s}$  and the CP contact time was 2 ms with 8 s of acquisition time delay.  $^{15}\text{N}$  chemical shifts were referenced to external solid ammonium chloride  $^{15}\text{NH}_4\text{Cl}$  (95%  $^{15}\text{N}$ -enriched). In order to convert these data into the nitromethane scale, the relation  $\delta(\text{CH}_3^{15}\text{NO}_2) = \delta(^{15}\text{NH}_4\text{Cl}_{\text{cryst}}) - 338.1 \text{ ppm}$  may be used.<sup>36</sup>

In the case of  $^{13}\text{C}$  experiment, the  $90^\circ$  pulse width was  $4.5 \mu\text{s}$  with a contact time of 1 ms and acquisition delay of 6 s.  $^{13}\text{C}$  NMR spectra were referenced to glycine (Gly) as an external reference and then converted into the conventional TMS scale.

**REDOR Experiments.** The experiments were performed on a 4-channel 300 MHz Varian instrument using a homemade five-channel transmission line probe according to the design of Schaefer and McKay<sup>37</sup> equipped with a 4 mm spinning module. The characteristic frequencies of  $^1\text{H}$ ,  $^{13}\text{C}$ , and  $^{15}\text{N}$  nuclei were 299.98, 75.44, and 30.40 MHz, respectively. The rotor frequency was controlled to  $12\,000 \pm 4 \text{ Hz}$  employing a Varian MAS controller. The amount of cellulose in the sample was ca. 40 mg.

A detailed description of the REDOR method can be found elsewhere.<sup>34,38,39</sup> It measures the internuclear distance of a heteronuclear spin pair where the spins are coupled by the magnetic dipole–dipole interaction. The strength of this interaction is reciprocally proportional to the third power of the internuclear distances. In our experiments the heteronuclear  $^{13}\text{C}$ – $^{15}\text{N}$  dipolar coupling was analyzed. The integral intensities of spectral lines in  $^{13}\text{C}$  CPMAS NMR spectra were compared; they were obtained without and with the recoupling of the  $^{13}\text{C}$ – $^{15}\text{N}$  dipolar interaction using rotor synchronized pulses applied to both spins.

## Results

**NMR Characterization of L-Lysine-Functionalized Cellulose.** The presence of amino acids in all the cellulose-modified samples was qualitatively evaluated by means of the classical ninhydrin color test.<sup>6</sup> When a mixture of ninhydrin and modified cellulose is heated, it turns to purple-blue. The observed effect is caused by the formation of Ruhemann's Purple, which is the product of the reaction of ninhydrin with the  $\alpha$ -amino group of L-lysine. Elemental analysis was used to determine the degree of the cellulose functionalization. All samples contained one L-lysine-functional group per four AGU units.

$^{15}\text{N}$  CPMAS NMR spectra of LysCel,  $[\alpha\text{-}^{15}\text{N}]$ LysCel, and  $[\varepsilon\text{-}^{15}\text{N}]$ LysCel are depicted in Figure 1. As the CP technique was used, relative signal intensities within each spectrum do not correspond to the relative amount of the different nitrogen sites. The selective labeling used helps to assign the peaks in Figure 1a. The nitrogen atoms of the aromatic ring resonate at 164 and 135 ppm which are tentatively assigned to positions 1, 5, and 3.  $\varepsilon\text{-}^{15}\text{N}$  resonates at 64 ppm and  $\alpha\text{-}^{15}\text{N}$  at 4 ppm. We recall that the  $\alpha$  nitrogen involved in a peptide bond resonates at ca. 87 ppm.<sup>40</sup> The spectra in Figure 1a,b do not contain any peak in this region. Thus, we can exclude the possibility of the cross-linking discussed in Scheme 2d.

**Solid-State  $^{15}\text{N}$  and  $^{13}\text{C}$  CPMAS NMR Spectroscopy and Protonation States of Lyophilized L-Leucine and LysCel.** In order to correlate the  $^{15}\text{N}$  and  $^{13}\text{C}$  chemical shifts of aminocarboxyl groups with their protonation states, we have measured the natural abundant  $^{15}\text{N}$  and  $^{13}\text{C}$  CPMAS NMR spectra of L-leucine lyophilized at different pH. The results are depicted in Figure 2a,b and are summarized in Table 1, together with the assignments of the different protonation states.

The spectra can be explained in terms of solid mixtures of the different protonation states of L-leucine illustrated in Scheme

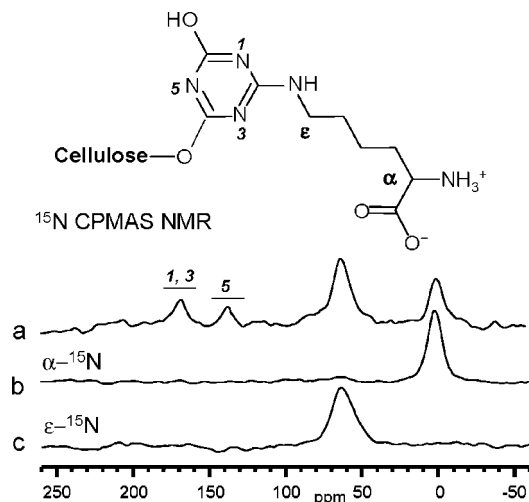


**Figure 1.**  $^{15}\text{N}$  CPMAS NMR spectra of LysCel: (a) natural  $^{15}\text{N}$  abundance L-lysine-, (b)  $[\alpha\text{-}^{15}\text{N}]$  labeled L-lysine-, and (c)  $[\epsilon\text{-}^{15}\text{N}]$  labeled L-lysine-functionalized cellulose.

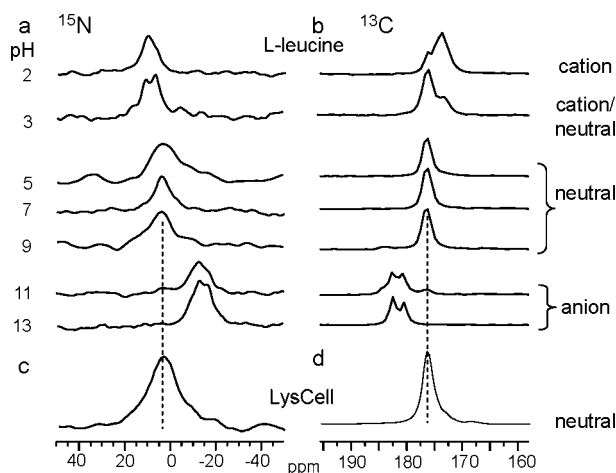


**Figure 2.** CPMAS NMR spectra of L-leucine lyophilized at different pH and of LysCel: (a)  $^{15}\text{N}$  and (b)  $^{13}\text{C}$  spectra of L-leucine at natural abundance; (c)  $^{15}\text{N}$  and (d)  $^{13}\text{C}$  spectra of  $^{13}\text{C}/^{15}\text{N}$ LysCel.

5. The cation is characterized by a high-field  $^{13}\text{C}$  and a low-field  $^{15}\text{N}$  signal, whereas the reverse is true for the anion. The neutral form adopts intermediate values. Around pH 2.5 both the cation and the neutral form are observed in slow exchange, and around pH 10 the neutral form and the anion. The signals of the anion are split into two components which indicate different anion sites. These observations indicate that in the solid state the mole fractions of the different protonation states correspond roughly to those found for aqueous solution, considering that L-leucine exhibits a  $\text{p}K_{\text{a}}$  value of 2.4 for the carboxylic acids group and of 9.7 for the ammonium group.<sup>41</sup>

In Table 1 are also included chemical shift values of leucine in water. The  $^{13}\text{C}$  chemical shifts behave qualitatively in a similar way as in the solid state, although the deprotonation shifts and the absolute chemical shift values are somewhat different. By contrast, the  $^{15}\text{N}$  chemical shift changes are different for the solid state and for aqueous solution. Such differences are not surprising in view of the different hydrogen bonded states of the aminocarboxyl groups in the solid state and in water.

In summary, we take the combination of the  $^{13}\text{C}$  and  $^{15}\text{N}$  chemical shifts values of 176 and 4.5 ppm obtained by lyophilization around pH 7 as diagnostic for the zwitterionic state of aminocarboxyl groups. It is then interesting to compare

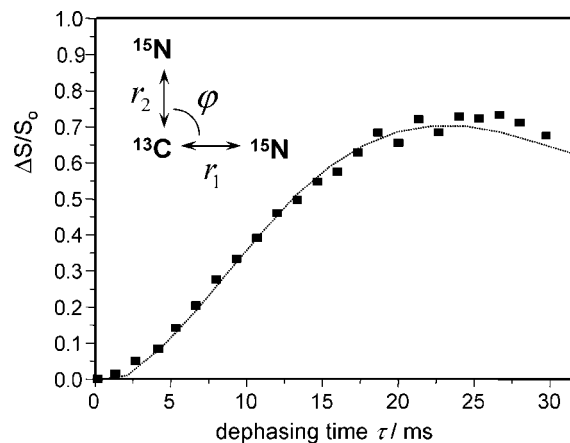


**Figure 3.**  $^{13}\text{C}\{^{15}\text{N}\}$  REDOR dephasing  $\Delta S/S_0$  as a function of the dipolar evolution time of the labeled-carbon peak of  $^{13}\text{C}/^{15}\text{N}$ LysCel. The solid line was calculated assuming that each carboxyl carbon atom site is connected to two nearest amino nitrogen atom sites ( $n = 2$  in Scheme 6), where the probability that an amino nitrogen site contains a  $^{15}\text{N}$  spin is  $1/2$ . The lengths of both carbon–nitrogen vectors were assumed to be equal and perpendicular to each other, i.e.,  $r_1 = r_2 = 3.5 \text{ \AA}$  and  $\phi = 90^\circ$ .

these values with those found for solid  $^{13}\text{C}/^{15}\text{N}$ LysCel whose  $^{13}\text{C}$  and  $^{15}\text{N}$  spectra are depicted in Figure 2c,d. Both the  $^{15}\text{N}$  and  $^{13}\text{C}$  signals are located at the positions where the neutral zwitterionic form of leucine resonates. This provides a strong evidence that the aminocarboxyl groups of LysCel are also zwitterionic and in close contact with each other.

**$^{13}\text{C}\{^{15}\text{N}\}$ REDOR NMR Study of Aminocarboxyl Interactions in LysCel.** The next problem was then to elucidate how the aminocarboxylic groups in LysCel interact with each other. To answer this question, we performed  $^{13}\text{C}\{^{15}\text{N}\}$ REDOR NMR experiments on solid  $^{13}\text{C}/^{15}\text{N}$ LysCel using  $^{13}\text{C}$  detection. This experiment consists of comparing the integral  $^{13}\text{C}$  signal intensity in two separate experiments as a function of the dephasing time  $\tau$ . In the REDOR experiment where pulses are applied to both types of spins, the  $^{13}\text{C}$  signal intensity  $S$  is reduced by dipolar dephasing in contrast to the normal or reference experiment where the intensity is labeled as  $S_0$ . The calculation of REDOR curves has been described previously.<sup>34,38,39</sup>

The results are depicted in Figure 3. The dipolar dephasing  $\Delta S/S_0 = (S_0 - S)/S_0$  is plotted as a function of the dephasing time  $\tau$ . The curve exhibits the typical behavior of a REDOR experiment.<sup>34,38,39</sup> At  $\tau = 0$  the signal intensities in both experiments are equal, and hence  $\Delta S = 0$ . As the REDOR signal dephases quickly in contrast to the reference signal,  $\Delta S/S_0$  increases, reaches a maximum of about 0.72 at a dephasing time  $\tau = 22 \text{ ms}$ , and then exhibits an oscillatory behavior for longer times.

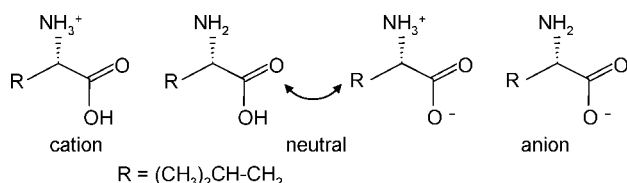
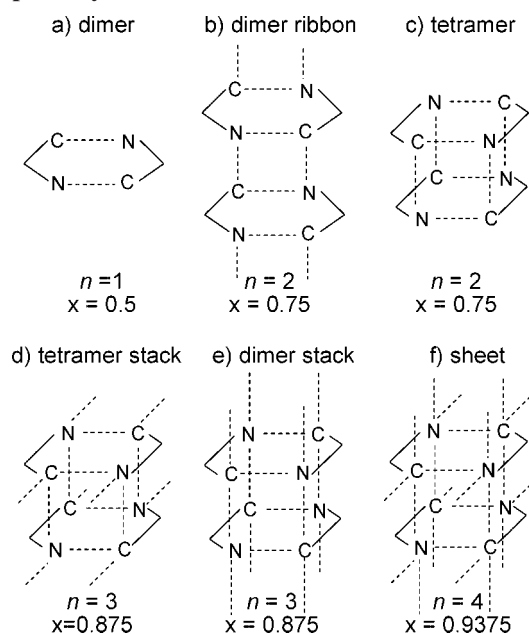
The REDOR curve of an isolated I-S-spin system is universal and depends only on the internuclear distance.<sup>37</sup> In an  $\text{IS}_n$  spin system, however, the evaluation of the REDOR experiment depends on the number of S-spins coupled to the observed I-spin, their distances, and their relative orientations. In this case, the REDOR dephasing can be calculated by standard programs like SIMPSON<sup>42</sup> or alternatively by optimized MATLAB routines,<sup>43,44</sup> which allow a faster fitting of the experimental data. For the simulations a structural model of the system is made and the geometry parameters of this model are optimized to fit the REDOR curve.

Owing to the geometry of the cellulose backbone and the lysine side chains, we can restrict ourselves in the evaluation of the REDOR data to nuclei in the first coordination sphere of

**TABLE 1:**  $^{15}\text{N}$  and  $^{13}\text{C}$  Chemical Shifts of Lyophilized Solid L-Leucine and [ $^{13}\text{C}/^{15}\text{N}$ ] LysCel

pH <sup>a</sup>	lyophilized solid L-Leucine		L-leucine in water		assignment
	$\delta(^{15}\text{N})/\text{ppm}$	$\delta(^{13}\text{C})/\text{ppm}$	$\delta(^{15}\text{N})/\text{ppm}$ <sup>47,48</sup>	$\delta(^{13}\text{C})/\text{ppm}$ <sup>49</sup>	
2	11	173.6	-4	170	$\text{Cl}^- \text{NH}_3^+ \text{CHRCOOH}$
3	7 to 11	176.2/173.6	—	—	$\text{Cl}^- \text{NH}_3^+ \text{CHRCOOH}$
5	4 to 5	176.2	—	—	$\text{NH}_3^+ \text{CHRCOO}^-$
7	4 to 5	176.2	-3	172	$\text{NH}_3^+ \text{CHRCOO}^-$
9	4 to 5	176.2	—	—	$\text{NH}_3^+ \text{CHRCOO}^-$
11	-12 to -16	180.7/182.7	-11	181	$\text{NH}_2 \text{CHRCOO}^- \text{Na}^+$
13	-12 to -16	180.7/182.7	—	—	$\text{NH}_2 \text{CHRCOO}^- \text{Na}^+$
[ $^{13}\text{C}/\alpha\text{-}^{15}\text{N}$ ] LysCel					
7	5 to 4	176.2			$\text{NH}_3^+ \text{CHRCOO}^-$

<sup>a</sup> pH of lyophilization.  $\delta(^{13}\text{C})$  and  $\delta(^{15}\text{N})$  in ppm. Solid -state  $\text{p}K_a(\text{NH}_3^+) \approx 10$ ,  $\text{p}K_a(\text{COOH}) \approx 2.5$ .

**SCHEME 5: Protonation States of L-Leucine****SCHEME 6: Possible Assemblies of Aminocarboxyl Groups in LysCel<sup>a</sup>**

<sup>a</sup>  $n$  represents the number of nearest aminocarboxyl nitrogen sites for a given carboxyl carbon site as represented by the dashed lines. The probability  $p$  of finding a  $^{14}\text{N}$  spin in a nitrogen site is  $1/2$ . According to eq 1, this leads to a fraction  $1 - x = (1/2)^n$  of  $^{13}\text{C}$  spins which are not dipolar coupled to a  $^{15}\text{N}$  spin.

the I-spin and neglect the influence of nuclei which are more far away. The resulting possible dipolar coupling schemes of the aminocarboxyl groups for the simulation of our REDOR data are illustrated in Scheme 6a–f. C represents the carboxyl  $^{13}\text{C}$ -nuclei and N the amino  $^{15}\text{N}$ -nuclei of an aminocarboxyl group and the dashed lines sketch the relevant dipolar couplings.

The simplest case (Scheme 6a) is an isolated dimer, where each C can be dipolar coupled only to a single N and we have a simple IS-spin system ( $n = 1$ ). If the dimers are arranged as a flat ribbon with coplanar dimer planes (Scheme 6b), the result is an IS<sub>2</sub>-spin system ( $n = 2$ ). The same spin system is found for an isolated tetramer (Scheme 6c). By contrast, in the case of a stack of sandwich-packed tetramers (Scheme 6d) or dimers

(Scheme 6e), an IS<sub>3</sub>-spin system ( $n = 3$ ) and in the case of a sheet structure (Scheme 6f) an IS<sub>4</sub>-spin system ( $n = 4$ ) results.

Since the sample is prepared as a mixture of single- $^{13}\text{C}$ - and single- $^{15}\text{N}$ -labeled aminocarboxyl groups, the end value of the REDOR curve reflects the number of observed I-spins which are coupled to an S-spin. This is independent information in the determination of the spin system. If  $p$  represents the probability of finding a  $^{14}\text{N}$  spin in a neighboring nitrogen site,  $p^n$  is the probability of finding only  $^{14}\text{N}$  spin neighbors for a given spin system IS <sub>$n$</sub> . In this case the  $^{13}\text{C}$  signal is not dephased by dipolar coupling to  $^{15}\text{N}$ . The fraction of  $^{13}\text{C}$  spins dephased by dipolar coupling to  $^{15}\text{N}$  is then given by

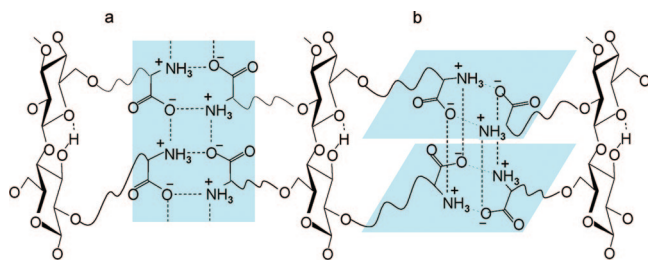
$$x = 1 - p^n \quad (1)$$

For the sample of [ $^{13}\text{C}/^{15}\text{N}$ ]LysCel studied here,  $p = 0.5$ . Thus, we obtain the values of  $x$  included in Scheme 6 for the different aminocarboxyl assemblies. In good approximation, the maximum of the REDOR dephasing curve in Figure 3, 0.72, is close to the value of  $x = 0.75$  revealing the IS<sub>2</sub> spin system ( $n = 2$ ) characteristic for an ideal dimer ribbon or for a tetramer. The final fitting of the REDOR curves was done with a laboratory written IS<sub>2</sub> spin system MATLAB routine<sup>43,44</sup> which uses purely heteronuclear  $^{13}\text{C}$ – $^{15}\text{N}$  couplings, based on the equations described in ref 45. In this case there are three structural parameters, namely the two dipolar couplings and the angle between the two dipolar vectors. The resulting best fit is shown as the solid line in Figure 3. It is obtained for an angle of  $\varphi = 90^\circ$  and identical CN distances of  $r_1$  and  $r_2 = 3.5 \text{ \AA}$ . For this parameter range there is only a weak dependence on the angle and on the size of the second coupling. Thus, a variation of  $\varphi$  in the range between  $\pi/3$  and  $2\pi/3$  or an increase of one of the distances up to  $4.0 \text{ \AA}$  does not change the fitting of the experimental data in a significant way. An example for  $r_1 = 3.5 \text{ \AA}$ ,  $r_2 = 4.0 \text{ \AA}$ , and  $\varphi = 60^\circ$  is given in the Supporting Information.

**Discussion**

By comparison with the  $^{13}\text{C}$  and  $^{15}\text{N}$  chemical shifts of neutral solid L-leucine exhibiting a network of zwitterionic aminocarboxyl groups, we obtained evidence for similar zwitterionic states of these groups in lysine-modified cellulose LysCel. In this material, half of the aminocarboxyl groups were labeled with  $^{13}\text{C}$  and the other half with  $^{15}\text{N}$  spins. This allowed us to obtain information about the assembly of the carboxyl groups in LysCel via dipolar  $^{13}\text{C}\{^{15}\text{N}\}$  REDOR NMR. We obtained evidence that a given aminocarboxyl group experiences two aminocarboxyl group neighbors. According to Scheme 6, this

**SCHEME 7: Proposed Structure of LysCel Exhibiting Zwitterionic Aminocarboxyl Groups: (a) Flat Dimer Ribbon; (b) Tetramers<sup>a</sup>**



<sup>a</sup> Both structures are compatible with the REDOR NMR experiments.

situation is typical for an assembly of aminocarboxyl dimers as is shown in Scheme 6b or in Scheme 6c, leading to structures which are illustrated schematically in Scheme 7. We note, however, that the data are compatible with disordered, nonideal structures. For example, the ribbons may be short and contain only a small number of dimers; an ideal ribbon may not be compatible with a disordered arrangement of glucose units in LysCel, although it is well established that cellulose is a highly ordered  $\beta$ -glucopyranose polymer.

Within the margin of error, the C $\cdots$ N distances between two aminocarboxyl groups of a dimeric substructure and between two neighboring aminocarboxyl groups in adjacent dimers are similar and about 3.5 Å. We note that this value coincides with the value found for zwitterionic solid glycine.<sup>22</sup> This observation consolidates the interpretation of all NMR data.

At present, we are not able to distinguish between the formation of Scheme 6b,c assemblies. Further insight into this problem could be gained by the application of homonuclear <sup>13</sup>C–<sup>13</sup>C recoupling techniques<sup>46</sup> which however are beyond the scope of this paper. However, we can exclude definitively isolated zwitterionic aminocarboxyl dimers as illustrated in Schemes 1 and 2. As was discussed in the Introduction, a zwitterionic state requires the presence of strong electric fields<sup>21</sup> which are generated either by surrounding polar solvent molecules such as water which are almost absent in dry LysCel or by the close presence of other dimers. This condition seems to be better fulfilled for the flat ribbon than for the tetramer. On the other hand, a ribbon requires a higher order, which may not be realizable in LysCel. Thus, an imperfect ribbon is the most plausible outcome of the present study.

Our results provide a plausible structural explanation on the experimental evidence exhibited by Allan et al.<sup>6</sup> which showed that amino acid modified cellulose fibers exhibited a 30% improvement, compared to untreated cellulose fibers, in the tensile strength of wet hand sheets of paper made with the amino acid modified material. However, this raises the following question. As mentioned in the experimental section, about a quarter of the anhydroglucose units (AGU) were modified on average with lysine groups, whereas the distances between the aminocarboxyl dimers in Scheme 7 indicate that neighboring AGU's are modified. This could be explained with a very unequal distribution of the modified and nonmodified AGU's within a sample. Thus, it is conceivable and very reasonable that the modified AGU's are all located on the surfaces of the fibers and the unmodified AGU's within the fibers.

## Conclusion

In this study we have examined using solid-state NMR the protonation state and the assembly of the aminocarboxylic groups in amino acid functionalized cellulosic fibers. L-lysine-

functionalized cellulose LysCel was used as a model system. We find that the aminocarboxylic groups in this material are in the zwitterionic state. This state is stabilized by an assembly into tetramers or a flat ribbon of dimers. Other assemblies such as dimer stacks or a sheet are not compatible with the NMR data. This structure is very different from structures of isolated amino acid dimers in the gas phase. This aminocarboxyl assembly seems to be attractive for applications in the future.

**Acknowledgment.** This work was supported by funds provided by the Secretariat of Public Education of Mexico under the program PROMEP/UdeG, the Deutsche Forschungsgemeinschaft, Bonn, the Fond der Chemischen Industrie, Frankfurt, the Russian Ministry of Education and Science (Project RNP 2.1.1.4139), and the Russian Foundation of Basic Research (Project 08-03-00615).

**Supporting Information Available:** The synthetic procedures are described in detail. This material is available free of charge via the Internet at <http://pubs.acs.org>.

## References and Notes

- Ott, E.; Spurlin, H. M. *Cellulose Part I, High Polymers*, 2nd ed.; Interscience Publishers, Inc.: New York, 1954; Vol. 5.
- Meshitsuka, G.; Isogai, A. Chemical Structures of Cellulose, Hemicelluloses and Lignines. In *Chemical Modification of Lignocellulosic Materials*; Hon, D. N. S., Ed.; Marcel Dekker, Inc.: New York, 1996; pp 11–34.
- Nissan, A. H. *Macromolecules* **1976**, *9*, 840–850.
- Page, D. H. *Tappi J.* **1969**, *52*, 674–681.
- Brown, K. C.; Mann, J. C.; Peirce, F. T. *J. Textile Inst.* **1930**, *21*, T187–204.
- Allan, G. G.; Delgado, E.; Lopez-Dellamary, F. A new interfibre system for paper involving zwitterions. In *Products of Papermaking*; Trans. 10th Fund. Res. Symp.; Baker, C. F., Ed.; Pira International: Leatherhead, Oxford, England, 1993; Vol. 2, pp 1101–1138.
- Bratskaya, S.; Schwarz, S.; Petzold, G.; Liebert, T.; Heinze, T. *Ind. Eng. Chem. Res.* **2006**, *45*, 7374–7379.
- Hubbe, M. A.; Rojas, O. J.; Lucia, L. A.; Jung, T. M. *Cellulose* **2007**, *14*, 655–671.
- Hubbe, M. A.; Jackson, T. J.; Zhang, M. *Tappi J.* **2003**, *2*, 7–12.
- Hubbe, M. A.; Moore, S. M.; Lee, S. Y. *Ind. Eng. Chem. Res.* **2005**, *44*, 3068–3074.
- Kanie, O.; Tanaka, H.; Mayumi, A.; Kitaoka, T.; Wariishi, H. *J. Appl. Polym. Sci.* **2005**, *96*, 861–866.
- Gruber, E.; Granzov, C.; Ott, Th. Cationization of Cellulose Fibres in View of Applications in the Paper Industry. In *ACS Symposium Series 688; Cellulose Derivatives (Modification, Characterization and Nanostructures)*; Heinze, T. J., Glasser, W. G., Eds.; American Chemical Society: Washington, DC, 1998; pp 94–106.
- Kircher, M.; Pfefferle, W. *Chemosphere* **2001**, *43*, 27–31.
- Delgado, E.; López-Dellamary, F. A.; Allan, G. G.; Andrade, A.; Contreras, H.; Regla, H. K. Cresson, T. *J. Pulp Pap. Sci.* **2004**, *30*, 141–144.
- Yamabe, S.; Ono, N.; Tsuchida, N. *J. Phys. Chem. A* **2003**, *107*, 7915–7922.
- Ding, Y.; Krogh-Jespersen, K. *Chem. Phys. Lett.* **1992**, *199*, 261–266.
- Locke, M. J.; McIver, R. T., Jr. *J. Am. Chem. Soc.* **1983**, *105*, 4226–4232.
- Strittmatter, E. F.; Wong, R. L.; Williams, E. R. *J. Am. Chem. Soc.* **2000**, *122*, 1247–1248.
- Gutowski, M.; Skurski, P.; Simons, J. *J. Am. Chem. Soc.* **2000**, *122*, 10159–10162.
- Chocholousová, J.; Vacek, J.; Huisken, F.; Werhahn, O.; Hobza, P. *J. Phys. Chem. A* **2002**, *106*, 11540–11549.
- (a) Golubev, N. S.; Denisov, G. S.; Smirnov, S. N.; Shchepkin, D. N.; Limbach, H. H. *Z. Phys. Chem.* **1996**, *196*, 73–84. (b) Ramos, M.; Alkorta, I.; Elguero, J.; Golubev, N. S.; Denisov, G. S.; Benedict, H.; Limbach, H. H. *J. Phys. Chem. A* **1997**, *101*, 9791–9800.
- Langan, P.; Mason, S. A.; Myles, D.; Schoenborn, B. P. *Acta Crystallogr.* **2002**, *B58*, 728–733.
- Drebushchak, N.; Boldyreva, E. V.; Shutova, E. S. *Acta Crystallogr.* **2002**, *E58*, o634–o636.
- Ferrari, E. S. *Cryst. Growth Des.* **2003**, *3*, 53–60.

- (25) Dawson, A.; Allan, D. R.; Belmonte, S. A.; Clark, S. J.; David, W. I. F.; McGregor, P. A.; Parsons, S.; Pulham, C. R.; Sawyer, L. *Cryst. Growth Des.* **2005**, *5*, 1415–1427.
- (26) Dalhus, B.; Görbitz, C. H. *Acta Crystallogr.* **1996**, *C52*, 1759–1761.
- (27) Görbitz, C. H.; Dalhus, B. *Acta Crystallogr.* **1996**, *C52*, 1754–1756.
- (28) Dalhus, B.; Görbitz, C. H. *Acta Crystallogr.* **1999**, *B55*, 424–431.
- (29) Bujdák, J.; Rode, B. M. *Catal. Lett.* **2003**, *91*, 149–154.
- (30) Meng, M.; Stievano, L.; Lambert, J.-F. *Langmuir* **2004**, *20*, 914–923.
- (31) Bismarck, A.; Aranberri-Askargorta, I.; Springer, J.; Lampke, T.; Wielage, B.; Stamboulis, A.; Shenderovich, I.; Limbach, H. H. *Polym. Compos.* **2002**, *23*, 872–894.
- (32) Tolstoy, P. M.; Schah-Mohammedi, P.; Smirnov, S. N.; Golubev, N. S.; Denisov, G. S.; Limbach, H. H. *J. Am. Chem. Soc.* **2004**, *126*, 5621–5634.
- (33) (a) Schimming, V.; Hoelger, C. G.; Buntkowsky, G.; Sack, I.; Fuhrhop, J. H.; Rocchetti, S.; Limbach, H. H. *J. Am. Chem. Soc.*, **1999**, *121*, 4892–4893.
- (34) Pan, Y.; Gullion, T.; Schaefer, J. *J. Magn. Reson.* **1990**, *90*, 330–340.
- (35) Kimura, S.; Naito, A.; Saitô, H.; Ogawa, K.; Shoji, A. *J. Mol. Struct.* **2001**, *562*, 197–203.
- (36) (a) Witanowski, M.; Stefaniak, L.; Szymanski, S.; Januszewski, H. *J. Magn. Reson.* **1977**, *28*, 217–226. (b) Srinivasan, P. R.; Lichter, R. L. *J. Magn. Reson.* **1977**, *28*, 227–234.
- (37) Schaefer, J.; McKay, R. A. U.S. Patent 5,861,748, 1999.
- (38) Gullion, T.; Schaefer, J. *J. Magn. Reson.* **1989**, *81*, 196–200.
- (39) Gullion, T. *Concepts Magn. Reson.* **1998**, *10*, 277–289.
- (40) Kricheldorf, H. R. *Org. Magn. Reson.* **1980**, *13*, 52–58.
- (41) Henchoz, Y.; Schappler, J.; Geiser, L.; Prat, J.; Carrupt, P. A.; Veuthey, J.-L. *Anal. Bioanal. Chem.* **2007**, *389*, 1869–1878.
- (42) Bak, M.; Rasmussen, J. T.; Nielsen, N. C. *J. Magn. Reson.* **2000**, *147*, 296–330.
- (43) Macholl, S.; Börner, F.; Buntkowsky, G. *Z. f. Phys. Chem.* **2003**, *217*, 1473–1505.
- (44) Macholl, S.; Börner, F.; Buntkowsky, G. *Chem. Eur. J.* **2004**, *10*, 4808–4816.
- (45) Goetz, J. M.; Schaefer, J. *J. Magn. Reson.* **1997**, *127*, 147–154.
- (46) Bennett, A. E.; Griffin, R. G.; Vega, S. *NMR Basic Principles and Progress*; Springer Verlag: Berlin, 1994; Vol. 33, pp 1–77.
- (47) Naullet, N.; Tome, D.; Martin, G. J. *Org. Magn. Reson.* **1983**, *21*, 564–566.
- (48) Leipert, T. K.; Noggle, J. H. *J. Am. Chem. Soc.* **1975**, *97*, 269–272.
- (49) Surprenant, H. L.; Sarneski, J. E.; Key, R. R.; Byrd, J. T.; Reilley, C. N. *J. Magn. Reson.* **1980**, *40*, 231–243.

JP8081968